Sensors & Transducers, Vol. 251, Issue 4, April 2021, pp. 11-18

Sensors & Transducers

Published by IFSA Publishing, S. L., 2021
http://www.sensorsportal.com

EEG Real Time Analysis for Driver's Arm Movements Identification

[*] Enrico Zero, Chiara Bersani and Roberto Sacile

Department of Informatics, Bioengineering, Robotics and Systems Engineering, University of Genova, Via all'Opera Pia 13, 16145 Genova, Italy

E-mail: enrico.zero@dibris.unige.it

Received: 22 January 2021 /Accepted: 3 April 2021 /Published: 30 April 2021

Abstract: Literature proved the potential benefits of autonomous vehicles in terms of road safety, traffic congestion, and energy consumption. The autonomous vehicles must be supported by advanced sensors and technologies to build reliable awareness of the external environment. However, cars with different levels of automation entail different levels of human intervention during the driving tasks. In this context, the main issue is to determine the interaction between the human and the automated driving system which requires an exhaustive understanding of the driver behavior above all in critical situations. This paper presents a neural network-based classifier of EEG signals to identify the driver's arm movements by his/her brain electrical activities, when he/she must steer to perform a right or a left turn on a curvilinear trajectory. The classifier based on a time delay neural network (TDNN) aims to classify the human's EEG signals when the participant executes the action to move his/her arms gripping a real steering wheel while driving in a simulated environmental. The performances of the classifier related to the recognition of the driver's arm movements by the brain signals demonstrated promising results that are worthwhile to be further explored.

Keywords: EEG, Identification, Neural network, Autonomous vehicles, Safety.

1. Introduction

In the automotive context, research and innovation have recently focused on the realization of self-driving vehicles. Autonomous Vehicles (AV) refer to car which can detect the environment by devices and sensors installed on board and to drive with a limited or without human intervention. According to the SAE International Standard 0, AVs are classified in six different levels of automation, from level 0 where the driver is the only decision maker to the forthcoming level 5 where the vehicle is completely managed by the automated driving systems (ADS). In detail, at level 0, the driver performs all dynamic driving tasks (DDTs) which consist in the tactical and operational functions required for the vehicle motion. Level 1 is applied when the ADS performs the DDTs related to either the longitudinal or the lateral vehicle motion control. At level 2, the ADS performs, simultaneously, both the longitudinal and the lateral vehicle control. At level 3, the ADS also performs the Object and Event Detection and Response (OEDR) to identify and to avoid events or obstacles on the route. At level 4, the ADS also completes DDT fallback 0. This function consists in a higher automation equipment which may intervene when the ADS fails in case of risk conditions. In the low levels of automation (Level 0 to Level 2), the driver is considered present and essential to compute part of the main DDTs. In the level 3, the driver may assist the ADS when a failure occurs during a trip, while at the level 4, the ADS performs overall function included the DDT fallback. Level 5 is reached when the vehicle is fully autonomous without the human user's intervention.

To detect and to identify the external environment, the ADS must recognize in real time the road shape, road signs, and the different objects on the road 0. For this reason, the AV must be equipped with specific sensors such as camera, Radar or Light Detection and Ranging (LiDAR) 0. The recent technological advances in the image treatments provides object-detection models based on multiclass problems where the different elements which can appear on the road may be recognized. In 0, a 2D object detection model for vehicles, pedestrian and cyclist identification is proposed. The authors compared both one and two stages deep learning techniques to process images with different resolutions to identify the method which generates the best trade-off between speed and accuracy for the detection system. In 0, the authors proposed a radar-based deep neural network (DNN) to recognize road segmentations when the different objects such as road-users, obstacles, and other obstructions are present on the street.

So, the use of radar and camera fusion algorithm provides better performances in respect to one sensor application above all in severe environmental condition 0. The LiDAR represents the main expensive solution among the detection systems whether, due its high resolution, is also the most adequate, above all, for SAE level 4 and 5. The 3D LiDAR provides images and measurements not affected by sunlight and different classifier have been tested for the real time obstacle detection. Among others, support vector machine (SVM) is used in 0 to recognized in real time vehicles on an urban context while a convolutional neural network has been adopted to classify vehicle lane change through LiDAR-based environment analysis 0.

1.1. EEG Based Driver Behavior Detection

In AVs at level 5, the driver is completely absent in the decision framework. To reach this condition, the vehicle must drive in an autonomous way. A propaedeutic analysis of the driver behaviour must be carried out to define the traditional driving style and to identify the relationships between the automated and non-automated driving system in order to implement the control commands at the operational level. In literature it is demonstrated that the physical and neurological driver's state affects the driving performances 0. The physiological state of the driver may be detected by different modalities based on the electrooculogram (EOG), the functional magnetic resonance imaging (fMRI), the high-frequency electrocardiogram (ECG) or the electroencephalography (EEG).

Driver's fatigue and distraction represent the major causes of accidents and crashes. In 0, the EOG, which detects the electrical signal generated by eye movements, is acquired, and processed by the fusion technique to identify driver's drowsiness. The fMRI identifies changes in cerebral oxygenation during cognitive tasks and it is used to demonstrate the correlation between brain activation and simulated driving actions 0. In a similar way, in 0, the authors applied a functional near infrared spectroscopy (fNIRS) to quantify variations in cortical activity related to changes in workload during driver tasks. Several studies monitored the heart rate variability to extract significant features related to driver drowsiness 0, driver workload 0 or sleepiness 0.

The EEG monitoring refers to the acquisition of brain signals from the different lobes of the brain in order to identify the cerebral waves variations when the subjects perform cognitive task. The EEG signals represent one of the main promising and reliable physiological indicators to describe human state 0. The EEG recording is often used to evaluate driver attention 0, fatigue 0, mental state 0 or, in general, cognitive response in driving environment 0. More recently, the EEG signal acquisition has also been used to identify the human intention for movements. The main objective of this research field, in the context of the AV, is to extract the main features from the EEG signals while the driver performs a specific movement and to classify the brain activities as belonging to the subject's intention to move the related part of his/her body.

Traditionally, the EEG device and the classification algorithm are coupled to a Brain Computer Interface (BCI) system. The EEG based BCI provides the possibility for the user to command an external device through the brain electrical signals according to his/her intention. In other words, the EEG acquires the cerebral signals, the classifier interprets the human movement intentions by the brain activities and finally the BCI translates them into a command for the devices. An EEG based BCI may represent a novel sensor and transducer tool to identify the main parameters of a human movements such as speed, direction, and force 0. Special interest has been given to the classification of hands 0, fingers 0, and eyes movements 0. In 0, a review about detection of movement intention using EEG signals appears.

Although the EEG based BCI may be a significant improvement in the realization of tools which assist the driver to prevent accidents, limited literature appears in the context of arm movements identification. In 0, the authors developed a classifier based on the support vector machine (SVM) to classify three classes of driver movements, left, right and brake. By the proposed approach, the authors obtained to predict the driver's action 500ms earlier with an accuracy of 94,6 %. Also, in 0, SVM and convolutional neural networks (CNN) are applied to EEG signals acquired during a breaking action to detect pedal pushing and to discriminate between driver's intent to brake in emergency condition and in the normal state of driving. In those experiments, the average accuracy reaches about 71 %. In 0, the authors used EEG signals and waveband specular meteor radar (SMR) to monitor drivers' physiological state and eye-movement electrical waves to identify the relationship between driver fatigue states and driver's grip force on the steering wheel while driving.

More recently, the EEG based BCI are used in the closed loop to establish a communication to external devices and send command inputs to them. Furthermore, imagined movement decoding methods are successfully used to classify horizontal and vertical movements of the right arm using EEG 00. In 0, the authors implemented a quadratic discriminant analysis (QDA) method to generate a classifier tested to regulate the motion of brushless DC motor used in neuro-aid engineering application. In this case, two classes are identified from EEG features to move the motor in clockwise and anticlockwise directions. Similar applications based on EEG signals for motor imagery classification appear in literature related to hand prostheses 0, wheelchair 0 or quadcopter 0. A wide review on robot controller by motor imagery BCI appears in 0.

This paper is inspired by 0 where a preliminary EEG based BCI is used to classify the arm movements of a driver who must rotate the steering wheel to perform a right or a left turn to execute a curve in a virtual driving environment. The main objective of this work is to increase the number of participants and extend the experiment results in terms of accuracy and reliability.

2. Material and Methods

This work focuses on a specific approach which aims at identifying and classifying the driver’s arm movements according to the data coming from the electroencephalography. In general, EEG systems are categorized as invasive and non-invasive. The first one included electrodes which have to be implanted inside the cranium while, in the second case, the electrodes may adhere to the scalp. In this work, the non-invasive solution is adopted.

2.1. Enobio EEG Cap

The experiments have been performed by using the Enobio Cap 8 Features. Signals were recorded at 500Hz from six different channels, namely F7, FZ, F8, C4, C3, CZ, in accordance with the international 10-20 system. The selected channels are shown in the Fig. 1.

The electrodes are located on the medial premotor area and on primary motor cortex.

2.1.1. Driving Test

The driving simulator consisted in two different components. Firstly, a common chair is positioned in front of an LCD screen which projected the driving simulated environment. Besides, the user is also provided with a steering wheel connected to the pedal system to perform real movements for turning and breaking.

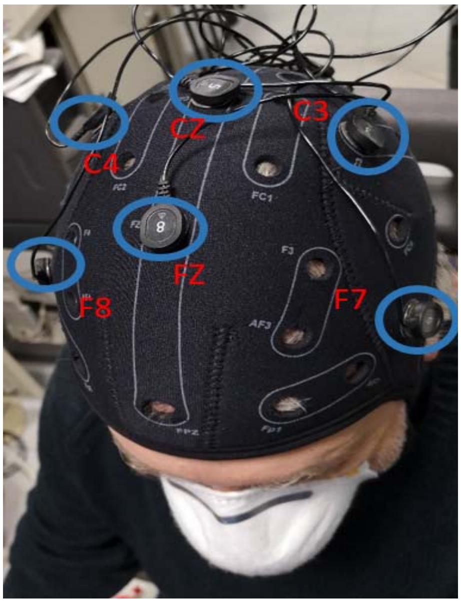

Fig. 1. Electrodes placement in the ENOBIO cap. (Blue circles represent the electrodes monitored during the experiments).

The set of subjects includes 3 participants who are, respectively, 25, 26 and 30 years old with driving license. Each participant performed three times the proposed test. The driver could rotate the steering wheel, accelerate or brake as if he/she were driving a real car. Each simulation lasted 15 minutes and, the user had to drive along a tour represented by the Fig. 2.

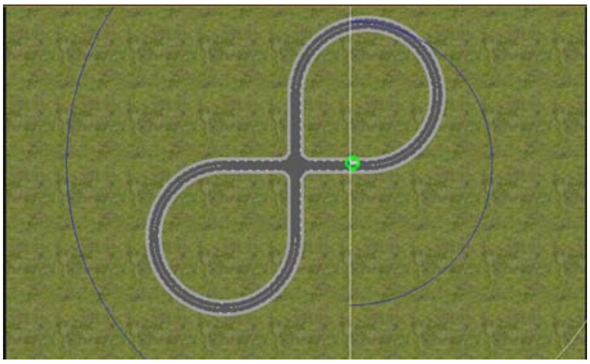

Fig. 2. Test drive circuit in OKTAL Simulator environment.

In each test, each driver run almost eight times on such route. OKTAL Scanner Studio is the software used to generate the simulation environment. The focus of this paper is to study the correlation between the arm movements of the driver while performing the right/left curves on the road and the related recorded EEG signals.

2.2. Preprocessing Data

The elaboration data was performed in Matlab R2020b. A high pass filter to 0.167 Hz was applied to the EEG signals to remove the direct current shift. Three different analyses have been realized by the implementation of time delay neural network (TDNN). TDNN has been used due to its capability to generate a finite dynamic response to time series input data.

The TDNN is typically successfully used in complex input-output identification but its large application in EEG signal analysis has been verified due to the non – stationary nature of the brain activities 0. In 0 the TTDN is applied for the classification of finger movements with a recognition rate of 93.02 %.

The TDNN performed in this paper, whose structure is presented in the Fig. 3, has 10 time delays and 4 hidden units.

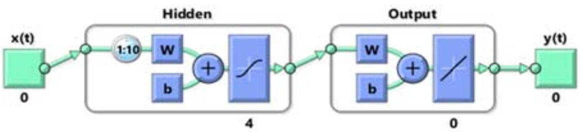

Fig. 3. TDNN used in the paper.

2.3. Experiments

The experiment involved 3 measurement sessions for each participant, once in three different days. In the following, the data are identified by the participant ID, P1 or P2 or P3, and by the training sessions chronologically numbered as 1, 2 or 3. Three different analyses have been carried out on the monitored EEG signals.

2.3.1. First Analysis

The first test is related to the classifier generation by the Levenberg Marquardt algorithm based TDNN. The data acquired in each session for each participant was divided in two an equal number of samples, labelled as 1A, 1B, 2A, 2B, 3A, 3B. The different sets of data have been used to train and test six TDNNs in order to identify the best classifier in term of correlation.

In Table 1, the different training and test datasets used in the applications appear.

Table 1. Set of data used to train and test the TDNNs in the first analysis.

TDNN	Training set	Test set
NN1	1A	1B
NN2	2A	2B
NN3	3A	3B
NN4	2A, 2B, 3A	3B
NN5	1A, 1B, 2A	2B
NN6	1A, 1B, 2A, 2B, 3A	3B

The generated NNs listed in Table 1 have been realized for each participant creating 18 TDNNs (6 NNs for the three participants). The main objective of the first analysis is to evaluate if the increasing number of input data in the training phase may reflect a better recognition performance.

2.3.2. Second Analysis

In the second test, the TDNNs, obtained in the previous test, have been modified. In particular, the NN4, NN5 and NN6, for each participant, have been revised by modifying the cost function which minimizes the Mean Square Error (MSE). In this second approach, a weight p_i has been introduced, for each sample which belongs to the training set, in the objective function as in (1).

$$MSE = \frac{1}{N * S} \sum_{k=1}^{S} \sum_{i=1}^{N} p_i^s \, (y_i^s - \hat{y}_i^s)^2, \qquad (1)$$

where:
MSE =mean square error;
S = number of dataset *s-th* used in the training;
N = number of elements in each dataset *s-th* used in the training set;
p_i^s = weight associated to each data *i-th* belonging to the dataset *s-th*;
y_i^s = observed value of the output in the dataset *s-th*;
$\hat{y}_i^s$ = predicted value for the output in the dataset *s-th*.

The new TDNNs, namely NN7, NN8 and NN9, are trained and tested by the same data set already adopted, respectively, in NN4, NN5 and NN6 for each participant. However, in this new approach, the objective functions for the training phase have been modified balancing the different input components as appear in Table 2. Note that the data coming from the older tests have lower weights with respect to the recent ones.

Table 2. TDNNs characteristics.

TDNN	Dataset *s-th* in the objective function	Weights p_i^s	Test set
NN7	2A	0.5	3B
	2B	0.5	
	3A	1	
NN8	1A	0.5	2B
	1B	0.5	
	2A	1	
NN9	1A	0.25	3B
	1B	0.25	
	2A	0.5	
	2B	0.5	
	3A	1	

The aim of the second analysis is related to identify the set of parameters which, by multiplying the objective components, increase the accuracy of the recognition.

2.3.3. Third Analysis

The non-linear characteristics of the neural network function may keep the results to be sensibly different according to the initialization of the weights present in its units. The third test has been carried out to evaluate TDNN performance variations according to different initializations of the values of the weights related to the layers of the neural network, calibrated or randomized.

Specifically, the performances have been evaluated comparing the TDNN recognition accuracy and the computational time required by the identification process, when the TDNN weights are randomly initialized by the system versus the TDNN weights initialized with values obtained from previous training sessions.

More specifically, in the latter case, values are calibrated according to the values obtained as output of the training phase for the TDNNs specified in the Table 3, column “Initialization of the weights of TDNN layers”. The columns “Training set” and “Test set” list, respectively, the dataset used to train and test the related NN in the row.

To explain better the approach, an example is presented. In the case of NN17, a standard TDNN has been created by a specific training on the samples 1A,1B, 2A related to the first and second sessions of experiments for the same participant. Then, the generated NN17, where the weights are initialized according to this first training phase, has been trained again on the subset 1A, 1B, 2A, 2B and tested on the subset 3A.

On the other hand, the NN16 is trained and tested with the same dataset of NN17 but without specific values of the weight parameters.

3. Results

Results are evaluated against two main indicators, *MSE* and *R*, which is the correlation coefficient of the predicted versus the actual values.

A preliminary analysis about the values for *R* and the *MSE*, for the TDNNs generated for the three participants is displayed in Table 4.

The results demonstrated that the *R* value, averaged over the three participants for the overall generated TDNNs, is close to 0.5. Also, the *MSE* values represent promising results in terms of reliability for the proposed approaches.

Table 5 shows the *R* index of each TDNN in the first analysis for the second participant (P2).

The results show a sensible good correlation between the EEG signals and the actual arm movements of the participant. In three cases, R is greater than 0.6.

From Table 1, it is possible to note a growing number of datasets used to train the NNs, from NN1 to NN6. However, by the results in Table 5, the increasing number of input data for the training phase does not reflect a significant improvement of the performances in terms of *R* and *MSE*.

Table 3. Generation of the weights used in the TDNNs.

TDNN	Initialization of the weights of TDNN layers	Training set	Test set
NN10	weights generated by 1A, 1B, 2A, 2B	3A	3B
NN11	weights generated by 1A, 1B	2A	2B
NN12	random weights	1A, 1B	2A
NN13	weights generated by 1A	1A, 1B	2A
NN14	random weights	1A, 1B, 2A	2B
NN15	weights generated by 1A and 1B	1A, 1B, 2A	2B
NN16	random weights	1A, 1B, 2A, 2B	3A
NN17	weights generated by 1A, 1B, 2A	1A, 1B, 2A, 2B	3A
NN18	random weights	1A, 1B, 2A, 2B, 3A	3B
NN19	weights generated by 1A, 1B, 2A, 2B	1A, 1B, 2A, 2B, 3A	3B

Table 4. Mean values of the performance indices computed for each TDNN averaged over the three participants.

TDNN	R	MSE
NN1	0.6812	0.4310
NN2	0.7001	0.4709
NN3	0.5603	0.5797
NN4	0.5818	0.5077
NN5	0.5348	0.6099
NN6	0.3836	0.6597
NN7	0.5950	0.5102
NN8	0.5774	0.5726
NN9	0.5364	0.5570
NN10	0.5811	0.5529
NN11	0.6316	0.5285
NN12	0.1001	1.0378
NN13	0.3802	0.8660
NN14	0.3917	0.7167
NN15	0.5169	0.6356
NN16	0.2713	0.7666
NN17	0.2132	0.8039
NN18	0.4379	0.6480
NN19	0.4075	0.6453
Mean	**0.48**	**0.64**

Table 5. First analysis results for P2.

TDNN	R	MSE
P2_NN1	0.6628	0.3838
P2_NN2	0.6610	0.4506
P2_NN3	0.5492	0.6213
P2_NN4	0.6435	0.4174
P2_NN5	0.2773	0.7922
P2_NN6	0.2907	0.7383

In the second analysis (Table 6), a stronger correlation is verified in the P2_NN7. Besides, the modified objective function produces better values, both for R and MSE, in the P2_NN8 versus the P2_NN5 and in the P2_NN9 versus the P2_NN6. In fact, respectively, the couple of NN5 and NN8 and the couple NN6 and NN9 are trained and tested by the same dataset for each participant but with different weight p_i^s (see Table 1 and Table 2).

In the third analysis, reported in the Table 7 related to the participant P2, the recognition accuracy for TDNNs initialized randomly or with accurate weights input values, appear very similar. The different approaches to initialize the layer parameters are not significant in terms of prediction. However, from the computation viewpoint, the TDNNs with accurate custom initialization appears, in general, less time expensive in respect to the ones with random initialization.

The three analysis are performed for the other two participants and, in the Table 8, the results regarding the first analysis in the first participant (P1) are reported.

Table 6. Second analysis results for P2.

TDNN	R	MSE
P2_NN7	0.6356	0.4363
P2_NN8	0.4851	0.6200
P2_NN9	0.4197	0.6080

Table 7. Third analysis results for P2.

TDNN	R	MSE	TIME (sec)
P2_NN10	0.6234	0.5489	47.0743
P2_NN11	0.4943	0.5873	34.6633
P2_NN12	0.2824	0.7039	241.2782
P2_NN13	0.4214	0.6526	205.9559
P2_NN14	0.1913	0.8688	451.9295
P2_NN15	0.3794	0.7182	185.1008
P2_NN16	0.3053	0.6668	418.4075
P2_NN17	0.0687	0.8356	276.9772
P2_NN18	0.3793	0.6414	245.0443
P2_NN19	0.1547	0.7996	583.0464

Table 8. First analysis results for P1.

TDNN	R	MSE
P1_NN1	0.8159	0.3657
P1_NN2	0.8538	0.2828
P1_NN3	0.6079	0.5130
P1_NN4	0.6486	0.4528
P1_NN5	0.8507	0.292
P1_NN6	0.6588	0.4622

For the first analysis, higher correlation is obtained in respect to the results reported for the P2. In this case, the value R is higher than 0.8 for NN1, NN2, and NN5.

In detail, Fig. 4 shows the comparison between the values related to actual angle associated to the rotation of the steering wheel realized by the participant during the simulation and the predicted values generated by the NN2 related to the direction of the arm movements. The graph highlights a significant overlapping of the peaks (values -1 and 1) associated to the correct prediction of the driver's arms movement on right and left.

The results related to second analysis regarding participant P1 are displayed in Table 9.

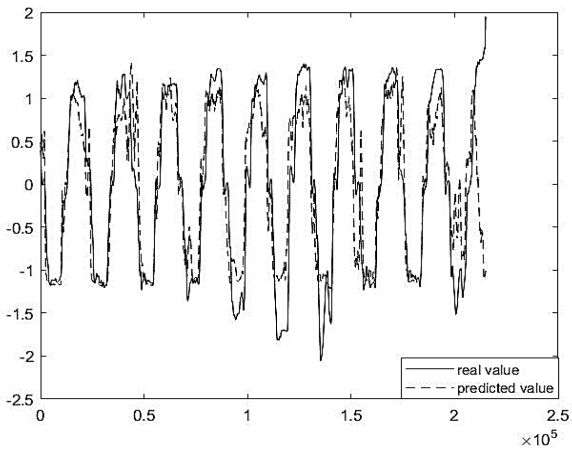

Fig. 4. Predictive and real value in P1_NN2.

Table 9. Second analysis results for P1.

TDNN	R	MSE
P1_NN7	0.6408	0.4633
P1_NN8	0.8502	0.2892
P1_NN9	0.6442	0.4464

In this case also, the R value is higher than 0.64 demonstrating a good correlation among predicted and actual data. On the contrary, the modified objective function does not introduce any positive variation in terms of prediction accuracy. The third analysis for P1 is reported in the Table 10.

Table 10. Third analysis results for P1.

TDNN	R	MSE	TIME (sec)
P1_NN10	0.6040	0.4949	100.052
P1_NN11	0.8517	0.2864	24.882
P1_NN12	0.4501	0.8698	114.260
P1_NN13	0.4696	0.7928	54.245
P1_NN14	0.8542	0.2854	196.969
P1_NN15	0.8495	0.2912	567.360
P1_NN16	0.5545	0.6188	442.865
P1_NN17	0.5983	0.5841	127.593
P1_NN18	0.6056	0.5841	209.203
P1_NN19	0.6392	0.4781	644.334

In this analysis, the R value is greater than 0.5 for 80 % of tests, while the MSE is lower than 0,5 for the 50 %. In general, anyway, we can conclude that the initialization of the weights for the neural network layers is not substantial in terms of accuracy of prediction in respect to the NNs randomly initialized.

4. Conclusions

This work aims at implementing a TDNN based classifier of EEG signals for driver's arm movements recognition.

This study is motivated by two principal purposes. Firstly, the driver's style recognition is crucial in the driving safety in order to prevent accidents and to react to critical situations. Secondly, the identification of the driver's behavior during specific driving tasks may support the understanding of the relationship between the driver and the automated driving systems (ADS), above all, in AVs at level 3 and 4.

The principal contribution of this paper is related to the development of a classifier for driver's arm movements recognition using EEG signals when the user rotates the steering wheel in order to perform a turn in a driving simulated scenario. The EEG data acquired by a non-invasive EEG cap, whose electrodes are in contact with the scalp, have been processed to classify those movements according to three classes: right or left turns and central position.

Moreover, three different methods have been implemented to evaluate possible improvements in the quality of the accuracy for the driver's arm movements prediction.

Firstly, the TDNNs generated for the recognition of movements have been modified by increasing the number of the datased used to train the NNs. In the second approach, the different components of the objective function have been differently weighted in order to minimize the MSE. Finally, the initialization of the weights associated to the layers of the neural network has been introduced to evaluate possible benefits in respect to the traditional random initialization.

Results demonstrated a statistically significant positive correlation of the EEG signals with the actual participant's actions to realize a turning in a car which cover a curvilinear path in a simulated environment. On the contrary, the proposed approaches to increase accuracy of movement's prediction do not assume specific relevance in the proposed experiments. So, due to the complexity of the problem and the relevance of the first preliminary analyses, this study merits to be further explored increasing the number of participants and evaluating new techniques for the classifier implementation.

Acknowledgements

This work is part of the Enrico Zero's PhD thesis. It has been partially sponsored by Eni.

References

[1]. SAE, Taxonomy and Definitions for Terms Related to On-Road Motor Vehicle Automated Driving Systems, J3016, SAE International Standard, 2014 https://www.sae.org/standards/content/j3016_201806/. Last access June 2020.

[2]. Xue W., Yang B., Kaizuka, T., Nakano K., A fallback approach for an automated vehicle encountering sensor failure in monitoring environment, in *Proceedings of the IEEE Intelligent Vehicles Symposium (IV)*, 2018, pp. 1807-1812.

[3]. Li D., Xu Q., An efficient framework for road sign detection and recognition, *Sensors & Transducers*, Vol. 165, Issue 2, February 2014, pp. 112-118.

[4]. Chavhan S., Kulkarni R. A., Zilpe A. R., Smart Sensors for IIoT in Autonomous Vehicles: Review, *Smart Sensors for Industrial Internet of Things*, Springer, Cham., 2021, pp. 51-61.

[5]. Carranza-García M., Torres-Mateo J., Lara-Benítez P., García-Gutiérrez J., On the Performance of One-Stage and Two-Stage Object Detectors in Autonomous Vehicles Using Camera Data, *Remote Sensing*, Vol. 13, Issue 1, 2021, 89.

[6]. Orr I., Cohen M., Zalevsky Z., High-resolution radar road segmentation using weakly supervised learning, *Nature Machine Intelligence*, Vol. 3, Issue 3, 2021, pp. 1-8.

[7]. Liu Z., Cai Y., Wang H., Chen L., Gao H., Jia Y., Li Y., Robust Target Recognition and Tracking of Self-Driving Cars With Radar and Camera Information Fusion Under Severe Weather Conditions, *IEEE Transactions on Intelligent Transportation Systems*, 2021.

[8]. Wang H., Zhang X., Real□time vehicle detection and tracking using 3D LiDAR, *Asian Journal of Control*, 2021.

[9]. Díaz-Álvarez A., Clavijo M., Jiménez F., Serradilla F., Inferring the Driver's Lane Change Intention through LiDAR-Based Environment Analysis Using Convolutional Neural Networks, *Sensors*, Vol. 21, Issue 2, 2021, 475.

[10]. Yan L., Wen T., Zhang J., Chang L., Wang Y., Liu M., Yan F., An Evaluation of Executive Control Function and its Relationship with Driving Performance, *Sensors*, Vol. 21, Issue 5, 2021, 1763.

[11]. Chieh T. C., Mustafa M. M., Hussain A., Hendi S. F., Majlis B. Y., Development of vehicle driver drowsiness detection system using electrooculogram (EOG), in *Proceedings of the IEEE 1st International Conference on Computers, Communications, & Signal Processing with Special Track on Biomedical Engineering*, November 2005, pp. 165-168.

[12]. Calhoun V. D., Functional Magnetic Resonance Imaging (fMRI), *Oxford Series in Human-Technology Interaction*, 2007, 51.

[13]. Bloomfield P. M., Green H., Gant N., Cerebral haemodynamics during simulated driving: Changes in workload are detectable with functional near infrared spectroscopy, *PLoS One*, Vol. 16, Issue 3, 2021, e0248533.

[14]. Murugan S., Selvaraj J., Sahayadhas A., Detection and analysis: driver state with electrocardiogram (ECG), *Phys Eng Sci Med*, Vol. 43, Issue 2, 2020, pp. 525–537 https://doi.org/10.1007/s13246-020-00853-8.

[15]. Perello-March J. R., Burns C. G., Woodman R., Elliott M. T., Birrell S. A., Driver State Monitoring: Manipulating Reliability Expectations in Simulated

Automated Driving Scenarios, *IEEE Transactions on Intelligent Transportation Systems*, 2021.

[16]. Salvati L., d'Amore M., Fiorentino A., Pellegrino A., Sena P., Villecco F., On-road detection of driver fatigue and drowsiness during medium-distance journeys, *Entropy*, Vol. 23, Issue 2, 2021, 135.

[17]. Lal S. K., Craig A., Boord P., Kirkup L., Nguyen H., Development of an algorithm for an EEG-based driver fatigue countermeasure, *Journal of Safety Research*, Vol. 34, Issue 3, 2003, pp. 321-328.

[18]. Lin C. T., Chuang C. H., Huang C. S., Tsai S. F., Lu S. W., Chen Y. H., Ko L. W., Wireless and wearable EEG system for evaluating driver vigilance, *IEEE Transactions on Biomedical Circuits and Systems*, Vol. 8, Issue 2, 2014, pp. 165-176.

[19]. Li W., He Q. C., Fan X. M., Fei Z. M., Evaluation of driver fatigue on two channels of EEG data, *Neuroscience Letters*, Vol. 506, Issue 2, 2012, pp. 235-239.

[20]. Zeng H., Yang C., Dai G., Qin F., Zhang J., Kong W., EEG classification of driver mental states by deep learning, *Cognitive Neurodynamics*, Vol. 12, Issue 6, 2018, pp. 597-606.

[21]. Lin C. T., Chung I. F., Ko L. W., Chen Y. C., Liang S. F., Duann J. R., EEG-based assessment of driver cognitive responses in a dynamic virtual-reality driving environment, *IEEE Transactions on Biomedical Engineering*, Vol. 54, Issue 7, 2007, pp. 1349-1352.

[22]. Robinson N., Chester T. W. J., Smitha K. G., Use of Mobile EEG in Decoding Hand Movement Speed and Position, *IEEE Transactions on Human-Machine Systems*, Vol. 51, Issue 2, 2021.

[23]. Robinson N., Guan C., Vinod A. P., Adaptive estimation of hand movement trajectory in an EEG based brain–computer interface system, *Journal of Neural Engineering*, Vol. 12, Issue 6, 2015, 066019.

[24]. Paek A. Y., Agashe H., Contreras-Vidal J. L., Decoding repetitive finger movements with brain activity acquired via non-invasive electroencephalography, *Frontiers in Neuroengineering*, Vol. 7, Issue 3, 2014.

[25]. Kim M., Kim B. H., Jo S., Quantitative evaluation of a low-cost noninvasive hybrid interface based on EEG and eye movement, *IEEE Transactions on Neural Systems and Rehabilitation Engineering*, Vol. 23, Issue 2, 2015, pp. 159-168.

[26]. Shakeel A., Navid M. S., Anwar M. N., Mazhar S., Jochumsen M., Niazi I. K., A review of techniques for detection of movement intention using movement-related cortical potentials, *Computational and Mathematical Methods in Medicine*, Vol. 2015, 2015.

[27]. Gougeh R. A., Rezaii T. Y., Farzamnia A., An Automatic Driver Assistant Based on Intention Detecting Using EEG Signal, in *Proceedings of the 11th National Technical Seminar on Unmanned System Technology 2019*, Springer, Singapore, 2021, pp. 617-627.

[28]. Hernández L. G., Mozos Ó. M., Ferrández J. M., Antelis J., EEG-Based Detection of Braking Intention Under Different Car Driving Conditions, *Frontiers in Neuroinformatics*, Vol. 12, 2018.

[29]. Li R., Chen Y. V., Zhang L., A method for fatigue detection based on Driver's steering wheel grip, *International Journal of Industrial Ergonomics*, Vol. 82, Issue 1, 2021, 103083.

[30]. Ofner P., Müller-Putz G. R., Using a noninvasive decoding method to classify rhythmic movement imaginations of the arm in two planes, *IEEE Transactions on Biomedical Engineering*, Vol. 62, Issue 3, 2015, pp. 972-981.

[31]. J.-H. Kim, Bießmann F., Lee S. W., Decoding three-dimensional trajectory of executed and imagined arm movements from electroencephalogram signals, *IEEE Transactions on Neural Systems and Rehabilitation Engineering*, Vol. 23, Issue 5, 2014, pp. 867-876.

[32]. Gupta G. S., Dave G. B., Tripathi P. R., Mohanta D. K., Ghosh S., Sinha R. K., Brain computer interface controlled automatic electric drive for neuro-aid system, *Biomedical Signal Processing and Control*, Vol. 63, 2021, 102175.

[33]. Owen M., Au C., The development of a brain controlled interface employing electroencephalography to control a hand prostheses, *International Journal of Biomedical Engineering and Technology*, Vol. 35, Issue 2, 2021, pp. 173-190.

[34]. Sulaiman N., Al-Fakih N. M. M. A., Rashid M., Jadin M. S., Mustafa M., Samsuri F., Offline EEG-Based DC Motor Control for Wheelchair Application, in *Proceedings of the 11th National Technical Seminar on Unmanned System Technology 2019*, Springer, Singapore, 2021, pp. 965-980.

[35]. A. S. Royer, A. J. Doud, M. L. Rose, B. He, EEG Control of a Virtual Helicopter in 3-Dimensional Space Using Intelligent Control Strategies, *IEEE Transactions on Neural Systems and Rehabilitation Engineering*, Vol. 18, Issue 6, Dec. 2010, pp. 581-589.

[36]. Zhang J., Wang M., A Survey on Robots Controlled by Motor Imagery Brain–Computer Interfaces, *Cognitive Robotics*, Vol. 1, 2021, pp. 12-24.

[37]. Zero E., Bersani C., Sacile R., EEG Based BCI System for Driver's Arm Movements Identification, *Automation, Robotics & Communications for Industry 4.0*, Vol. 77, 2021.

[38]. Rao R., Derakhshani R., A comparison of EEG preprocessing methods using time delay neural networks, in *Proceedings of the 2nd International IEEE EMBS Conference on Neural Engineering*, 2005. pp. 262-264.

[39]. Emayavaramban G., Ramkumar S., Amudha A., Kumar K. S., Classification of Hand Gestures Using FFNN and TDNN Networks, *International Journal of Pure And Applied Mathematics*, Vol. 118, Issue 8, 2018, pp. 27-32.

___